Jurnal Kejuruteraan 26(2014): 21-30

Sun Outage Calculator for Geostationary Orbit Satellites

(Kalkulator Gangguan Matahari untuk Satelit Orbit Pegun)

Jouko Vankka* & Antti Kestilä

ABSTRACT

Sun outages in satellite communication occur when the sun, a powerful broadband microwave noise source, passes directly behind the satellite (when viewed from Earth), causing the receiver with the beam directed towards the satellite to pick up the satellite signal and the noise from the sun. A new type of calculator was developed to accurately determine the occurrence of such phenomena for any chosen geostationary satellite and receiver location combination. The calculator outputs the degradation experienced by the satellite signal, enabling the receiver to take suitable countermeasures. The results from the calculator program were compared with measurement results and agreed to a good degree. Several different open-source calculation tools exist for sun outages. However, these tools are either built from incorrect assumptions or lack of a useful function, leading to inaccurate predictions for strength and beginning/ending time of the outages. The program described in this work has more inputs, such as the solar flux, with which the sun's activity can be considered when calculating outage duration and receiver noise temperature. Regression analysis was used to develop a linear model to estimate daily solar flux at a frequency of interest from the day's solar flux 2800 MHz observations (F10.7).

Keywords: Solar interference; sun outage; satellite communications

ABSTRAK

Gangguan matahari pada satelit komunikasi berlaku apabila matahari, satu sumber bunyi gelombang mikro jalur yang kuat, berlalu tepat di belakang satelit (apabila dilihat dari bumi) yang menyebabkan transponder penerima yang berada pada arah tepat kepada satelit akan menerima isyarat satelit dan gangguan daripada matahari. Sejenis kalkulator baru telahpun dibangunkan bagi menentukan ketepatan fenomena sebegini bagi mana-mana satelit geopegun dan lokasi transponder penerima yang dipilih. Kalkulator ini akan menunjukkan output kemerosotan yang dialami oleh isyarat satelit, di mana ia membolehkan transponder penerima mengambil langkah tindakan yang sesuai. Hasil yang diperolehi daripada program kalkulator ini telah dibandingkan dengan keputusan pengukuran dan bersetuju ke tahap yang baik. Terdapat juga beberapa alat pengiraan sumber yang berbeza untuk gangguan matahari. Walau bagaimanapun, alat-alat ini dibina sama ada daripada pengiraan yang kurang tepat atau kekurangan fungsi yang berguna, dan ini akan berlakunya jangkaan yang kurang tepat bagi kekuatan dan permulaan/ dan waktu berakhir gangguan tersebut. Program yang dinyatakan di sini mempunyai lebih input, seperti fluks solar, yang di mana dengan aktiviti matahari boleh diambil kira tatkala mengira tempoh gangguan dan suhu transponder penerima bunyi. Analisis regresi telah digunakan untuk membangunkan satu model linear bagi menganggarkan fluks solar harian pada frekuensi dari solar fluks pemerhatian harian 2800 MHz (F10.7).

Kata kunci: Gangguan solar; gangguan matahari; komunikasi satelit

INTRODUCTION

As shown in Figure 1, sun-related outages in satellite communications are caused by the sun's apparent passage behind satellites as seen from the earth stations receiving communications from them (Siocos 1973). This occurs around the vernal and autumnal equinoxes and lasts a few minutes daily over a period of a few days. The sun's energy interferes with the satellite's signal and affects the signals received by the earth station, which is referred to as sun transit, sun fade or solar/sun outage. The major effect of a sun outage is the increase of system noise temperature in the downlink direction of transmission (Garcia 1984, Johannsen 1988, Kivaria et al. 2011, Guo et al. 2012). The sun outage greatly affects transmission quality and limits system availability. Obviously, the ability of systems to operate through peak sun transit times is a function of the excess energy-per-bit to noise ratio ($\Delta E_b/N_0$) margin that was originally designed into the links (Song et al. 2010, Wenjuan & Peng 2010).

Several calculation tools exist in the public domain that can be used to predict the strength and/or duration of a solar outage between geostationary satellites and ground station locations (Sun Outage Calculator 2013; Telesat Sun Outage Calculator 2013). Using stronger channel encoding the earth station receiver can set up a high enough $\Delta E_b/N_0$

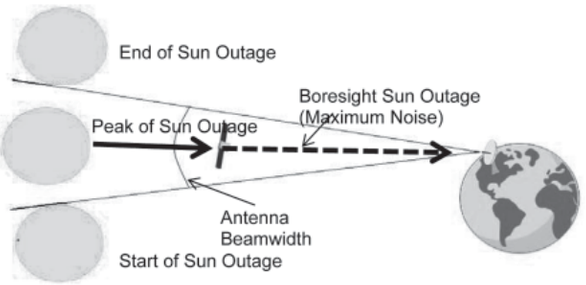

FIGURE 1. Sun outage

margin to keep the communication link going during the predicted sun outage. Several tools are missing important input parameters, which adversely affects the quality of the sun outage prediction. The calculator presented in this paper has several key inputs available, such as the solar flux, which enables more efficient calculation of sun outage duration and strength.

EFFECTIVE NOISE TEMPERATURE OF THE SUN

The sun's electromagnetic radiation at centimeter wavelengths is randomly polarized (Lyon & Mohammed 1998). Earth stations use a single polarization, commonly linear or circular, and receive only half of the incident radiation in the frequency band of use due to the blocking of the orthogonal polarization. The perceived solar brightness temperature is reduced by 3 dB as a result (Lyon & Mohammed 1998). The elevation in effective noise temperature as a result of the sun outage is equal to the weighted average of the sun's optical disc integrated over the received radiation pattern, multiplied by the polarization factor (p). The receiver antenna noise temperature (T_a) can be computed with the assumption that the sun is a disk of 0.5° diameter. The brightness temperature (T_S) at the receiver carrier frequency is assumed constant over the entire surface of the sun (Vuong & Forsey 1983).

$$T_a = \frac{pT_sG}{4\pi}\int_0^{\pi}\int_{\frac{-0.25\pi}{360}}^{\frac{0.25\pi}{360}} f(\theta^* - \theta_0^*)\,|\sin\theta^*|\,d\theta^* d\varphi^* \qquad (1)$$

where θ^* and ϕ^* are two of the three spherical coordinates expressed in radians integrated over the sun's solid angle; θ^*_0 is the antenna pointing offset (the angle between the center of the sun to the boresight direction of an antenna); and $f(\theta^*)$ is the antenna's gain pattern expressed as a power ratio. This can be estimated from the following Gaussian model

$$f(\theta^*) = e^{-6.10^{-5}(G-1)(360.\theta^*/(2\pi))^2} \qquad (2)$$

where G is the antenna's maximum gain

$$G = 109.66k\,D^2\,F^2 \qquad (3)$$

and k, D, F, and θ^* are, respectively, the antenna efficiency, antenna aperture diameter in meters, receive carrier frequency in GHz, and the off-axis angle from the antenna boresight axis (Vuong & Forsey 1983).

ESTIMATING SOLAR FLUX FROM OBSERVATIONS AT 2800 MHZ

Spectral shapes and magnitudes of the solar noise profile vary strongly with time and frequency (NGDC 2013). Typically, the solar flux density (*F10.7*) is measured at a wavelength of 10.7 centimeters (a frequency of 2800 MHz), because the *F10.7* is a good measure of general solar activity (Ho et al. 2008; Cakaj et al. 2005). This radio emission comes from the high part of the chromosphere and the low part of the corona (Ho et al. 2008, Bruevich et al. 2014). The National Geophysical Data Center (NGDC) web site (available at (NGDC 2013)) contains the long running time series of daily noontime radio flux measurements for the solar flux density values at the frequencies 245 MHz, 410 MHz, 610 MHz, 1415 MHz, 2695 MHz, 2800 MHz, 4995 MHz, 8800 MHz and 15400 MHz. Solar flux values (solar flux unit = 10^{-22} watt per square meter-hertz, symbol SFU) from January 1997 through February 2008 in Figure 2 are from Sagamore Hill (Massachusetts) and Dominion Radio Astrophysical Observatories (NGDC 2013). These data series have not been quality controlled and no monthly means are provided (NGDC 2013). Figure 2 illustrates the high level of interconnection between *SFU* values at frequencies 4995 MHz, 8800 MHz and 15400 MHz versus 2800 MHz (F10.7). There are two types of solar flux variations in Figure 2: long-term and short-term. The long-term variations include annual and 11-year solar cycle variations (Ho et al. 2008), while short-term variations usually refer to changes that take place within days. Figure 2 shows that the solar flux at 2800 MHz can change by a factor of 5.7 (from 65 SFU to 370 SFU) within two solar cycles.

Regression equations for *SFU* values at frequencies (245 MHz, 410 MHz, 610 MHz, 1415 MHz, 2695 MHz, 2800 MHz, 4995 MHz, 8800 MHz and 15400 MHz) vs. frequency (F) and *F10.7* (2800 MHz) are shown in

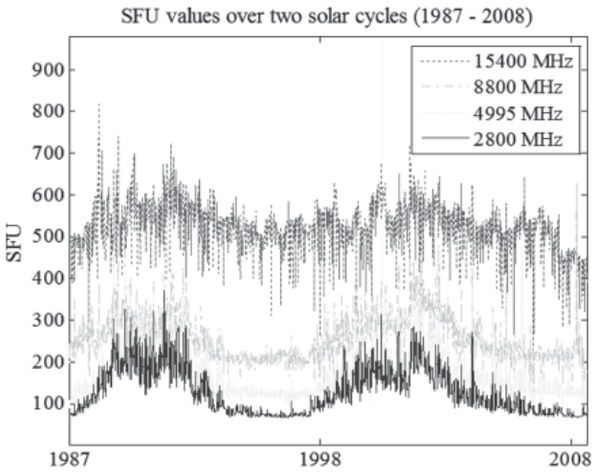

FIGURE 2. Interconnection between SFU values at different frequencies

TABLE 1. Regression equations for *SFU* values vs. frequency (*F* in MHz) and F10.7 (2800 MHz)

	Regression coefficients								
	a	*b*	*c*	*d*	*e*	*f*	*g*	*H*	R^2
$SFU = a + bF + cF10.7$	-52.31424	0.03134	0.61839						0.9570
$SFU = a + bF + cF10.7 + dF10.7 \times F$	-44.1362	0.02937	0.55458	1.5369×10^{-5}					0.9576
$SFU = a + bF + cF10.7 + dF10.7 \times F + eF^2 + fF10.7^2$	-39.6914	0.02211	0.65463	1.5369×10^{-5}	4.8594×10^{-7}	-3.3263×10^{-4}			0.9616
$SFU = a + bF + cF10.7 + dF10.7 \times F + eF^2 + fF10.7^2 + gF^3 + hF10.7^3$	0	0.047	0.55050	1.7280×10^{-5}	-4.4831×10^{-6}	6.9763×10^{-3}	2.2393×10^{-10}	-1.3536×10^{-5}	0.9706
$SFU = a + bF + cF10.7 + dF10.7 \times F$	28	-0.01	0.44	2.0×10^{-4}					0.5856

Table 1. The explained variation/total variation (R^2) value for the fitted regression will not give any significant enhancement with the addition of higher polynomial terms (see Table 1, last column). A method sometimes used for estimating solar flux from observations at 2800 MHz uses a formula proposed by Tapping (1994) (Mcgrath 2002). Tapping's formula does not seem to be a good method of estimating daily solar flux at a frequency of interest from the day's 2800 MHz observations due to the value of R^2 (0.5856; see Table 1 last row).

The solar flux density at any frequency *F* in MHz can be estimated by the following expression (linear model for 245 – 15400 MHz):

$$SFU = -52.31424 + 0.03134F + 0.61839\,F10.7 \qquad (4)$$

where *F10.7* is the current value of the solar radio emission at a frequency of 2800 MHz and one solar flux unit (*F10.7*) is 10^{-22} W m^{-2} Hz^{-1}. This value is measured and made available for example from the Dominion Radio Astrophysical Observatory in Penticton, Canada (NGDC 2013). The linear model from Equation 4 is fitted to the *SFU* values (from January 1997 through February 2008) at frequencies (245 MHz, 410 MHz, 610 MHz, 1415 MHz, 2695 MHz, 2800 MHz, 4995 MHz, 8800 MHz, and 15400 MHz) in Figure 3 with R^2 of 0.9570.

The solar brightness temperature (T_s) at frequency *F* in Hz is given in terms of the integrated flux density *SFU* by

$$T_s = \frac{SFUc^2}{2kF^2\Omega_s}, \qquad (5)$$

where *c* is speed of light (in vacuum 299.792.458 m/s), $k = 1.38 \times 10^{-23}$ J K^{-1} is Boltzmann's constant, and $\Omega_s = 6 \times 10^{-5}$ steradians is the mean solid angle subtended by the sun (Ho et al. 2008). Equation 5 is known as the Raleigh-Jeans law, which holds all the way through the radio frequencies for any reasonable temperature. The solar brightness temperature (T_s) follows the eleven-year sunspot cycle at radio frequencies

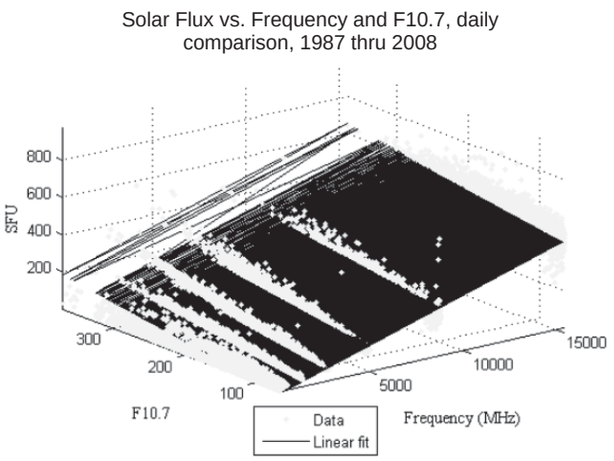

FIGURE 3. Linear fit from Equation 4: F10.7 and Frequency are fitted to SFU values at frequencies (245 MHz, 410 MHz, 610 MHz, 1415 MHz, 2695 MHz, 2800 MHz, 4995 MHz, 8800 MHz and 15400 MHz)

(see Figure 2); therefore, receiver antenna noise temperature (T_a) in Equation 1 is also periodic.

The $\Delta E_b/N_0$-degradation in dB at the receiver input can then be computed from the following (Vuong & Forsey 1983):

$$\Delta\left(\frac{E_b}{N_o}\right) = 10\log\left[\frac{T_{sys} + T_a}{T_{sys}}\right] \qquad (6)$$

where T_{sys} is the equivalent system noise temperature at the receiver input in the absence of a sun outage. T_{sys} includes the equivalent noise temperature of uplink noise, noise generated in the transponder, intermodulation and interference noise, downlink noise, and noise generated by the earth station's receiver, all of which are referred to the receiver input.

SIMULATIONS

PEAK ENERGY-PER-BIT TO NOISE RATIO DEGRADATION ($\Delta E_B/N_0$)

The energy-per-bit to noise ratio degradation is calculated from Equation 1-6 (Figure 4). The $\Delta E_b/N_0$ degradation increases with increases in antenna aperture diameter (increasing antenna gain from Equation 3), as shown in Figure 4. The sun is totally within the beam when the antenna's beam width is greater than the solar disk angular diameter (Figure 5). When the antenna aperture diameter is larger than 9 m and 15 m for the Ku-band and the C-band, respectively, the beam width is less than the solar disk angular diameter (Figure 5). The portion of the sun's surface covered by the antenna beam starts to decrease, but the higher antenna gain of the large antenna compensates for the effect of the decreasing collecting surface area (Equation 1). Therefore, $\Delta E_b/N_0$ degradation is nearly constant in Figure 4 for large antennas. The $\Delta E_b/N_0$ degradation also depends on the solar brightness temperature. For *F10.7* = 81 and *F10.7* = 250 solar flux units, the solar brightness temperature (T_S) from Equation 4 and Equation 5 at 12.5 GHz (Ku-band) is about 32% and 22%, respectively, of that at 4 GHz (C-band) because of the smaller wavelength. Therefore, the $\Delta E_b/N_0$ degradation is worse at the C-band than at the Ku-band for the same *F10.7* values when the $\Delta E_b/N_0$ degradation is nearly constant (Figure 4). The decreasing collecting surface area does not reduce the effect of the higher gain when the antenna beam width is larger than the solar disk angular diameter (for antenna diameters less than 8 m; Figure 4). Therefore the higher gain of the Ku-band antenna causes worse $\Delta E_b/N_0$ degradations. Even the solar brightness temperature is higher at the C-band for the same *F10.7* values.

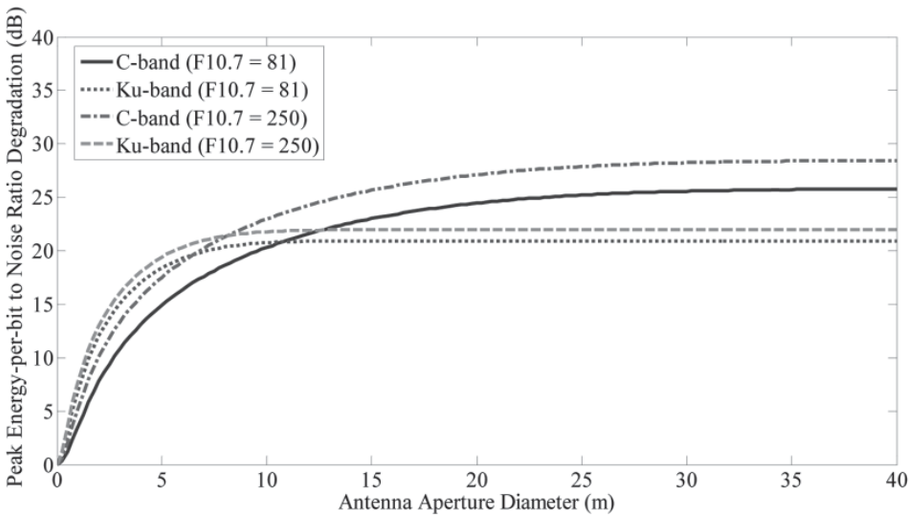

FIGURE 4. Maximum ΔEb/N0 degradation of the C-band and K_u-band with two F10.7 values (81 and 250 solar flux units) vs. antenna diameter. T_{sys} = 70 K in Equation 6; antenna pointing offset = 0 in Equation 1; k = 0.5 in Equation 3

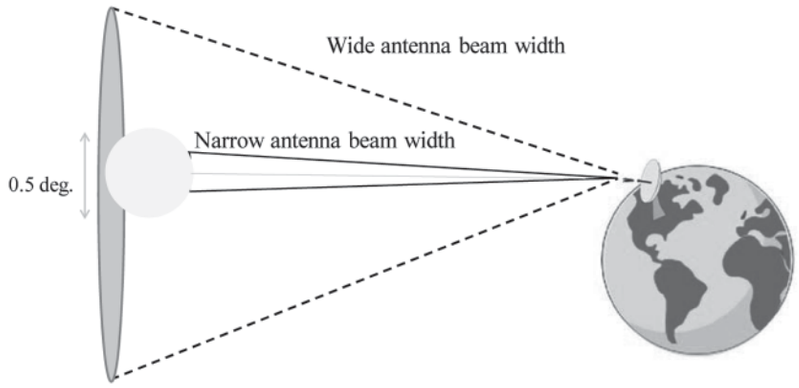

FIGURE 5. Geometry of antenna beams with two types of beam widths relative to the sun's angular diameter

$\Delta E_B/N_0$ DEGRADATION AS A FUNCTION OF ANTENNA POINTING OFFSETS

At the equinoxes, the solar motion is 0.4 degrees per day in declination, and thus even with an infinitely small antenna beam, the sun will still be in the beam for at least one day per equinox (Figure 6). The receiver antenna noise temperature caused by the sun greatly depends on antenna pointing offsets, the daily variations of which are shown in Figure 6. The $\Delta E_b/N_0$ degradation is shown in Figure 7 as a function of antenna pointing offsets in degrees. When the antenna beam points off the solar disk, $\Delta E_b/N_0$ degradation is reduced. The C-band receiver will have longer sun outage durations during the sun's transit than the Ku-band receiver (Figure 7). This can be explained by the narrower beam width of the Ku-band antenna.

Clearly, the ability of these systems to operate through peak sun outage times is a function of the excess $\Delta E_b/N_0$ margin that was originally designed into the links. To ensure continuity during times of sun outage, some additional margin in the downlink may be required when larger antennas are deployed (i.e. antennas 1.5 m and greater in diameter).

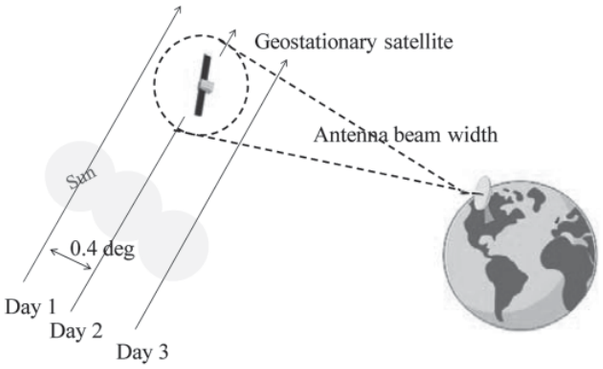

FIGURE 6. Transit of the sun through an antenna beam on successive days around the time of the equinox

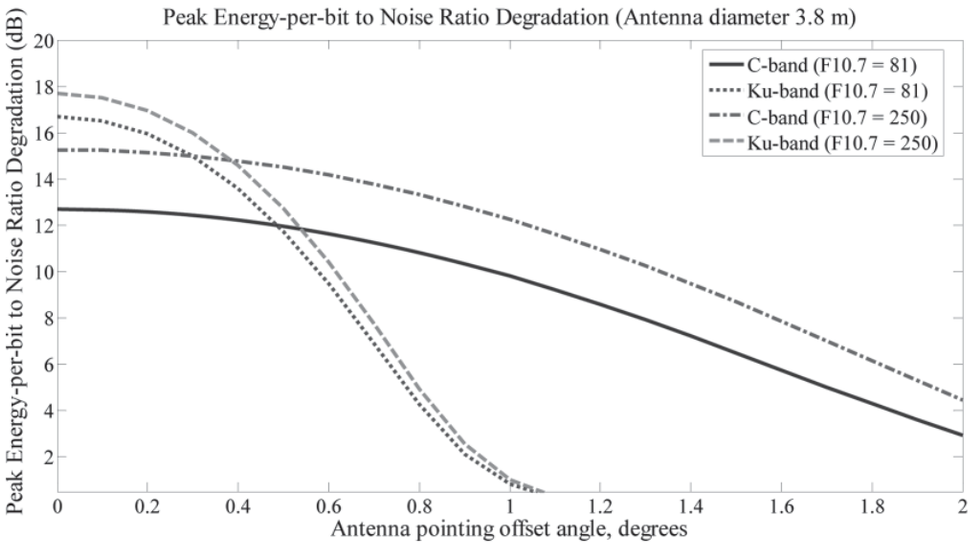

FIGURE 7. Maximum ΔEb/N0 degradation of the C-band and K_u-band with two F10.7 values (81 and 250 solar flux units) versus antenna pointing offset angle. T_{sys} = 70K in Equation 6; k = 0.5 in Equation 3. The half-power beam width of the antenna (3.8-m diameter) is 1.38° and 0.44° for the C-band and the Ku-band, respectively

SUN OUTAGE DURATION

The beam width of the receiving ground antenna, the solar flux density, and the margin in $\Delta E_b/N_0$ are the primary factors determining the duration of the sun outage and determine whether the receiver will experience a total communication outage or only a tolerable degradation in connection quality (Vankka 2013). The gain of the receiver antenna drops rapidly after the beam width angle approaches 3-dB, but does not go down to zero immediately. For this reason, if the sun is close to the receiver's 3-dB line it will affect the noise experienced by the receiver and degrade the communication link (Figure 8), making it difficult to define the exact times at which the sun outage begins and ends. However, the following equation can be used as an approximation (Figure 8):

$$Outage\ angle = \frac{6\sqrt{BW}}{Frequency \times Diameter} + 0.25°, \quad (7)$$

where *Frequency* is the downlink frequency in GHz, *Diameter* is the receiver parabolic reflector or dish antenna diameter in meters, and *BW* is the antenna beam width in decibels. If the $\Delta E_b/N_0$ margin is low and the solar flux density is high, then the beam width should be larger than 3 dB in Equation 7.

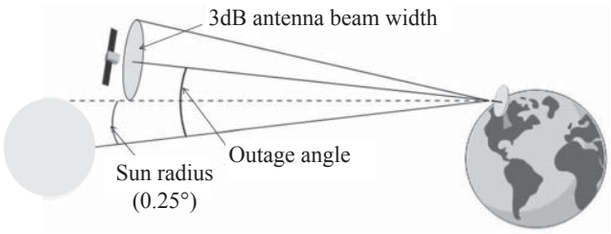

FIGURE 8. Outage angle

SUN OUTAGE CALCULATOR

OVERVIEW

Generality was the main goal behind the design of the calculator in this work. It makes as few assumptions as possible, and includes all important input parameters (see Figure 9), such as:

1. The satellite used
2. Up to two receiving ground stations
3. Season
4. Year
5. Receiver antenna diameter
6. Downlink frequency
7. Solar flux
8. System noise temperature
9. Outage angle
10. Polarization factor

As an output, it gives the start and end times (in universal coordinated time (UTC) and a user-defined local time) and durations with their respective $\Delta E_b/N_0$ degradations (Vankka 2013).

PROGRAM STRUCTURE

The sun outage calculator was written using the Java programming language, mainly due to its flexibility, ease, and extensive available libraries. The program consists of two different languages (Java and JavaScript) and their interface (Rhino) (Figure 10), and is structurally built from (Vankka 2013):

1. the main controlling program, written in Java;
2. three independent JavaScript function libraries for the main program;
3. NASA's JAT Java libraries; and
4. Rhino as an interface between Java and JavaScript.

The interface presented in Figure 9 was designed for simplicity and ease of use. The user fills in all the required data for the used satellite and the two receiver stations, and the output is printed to the large text box at the bottom-left. The user interface is based on a simple HTML-based

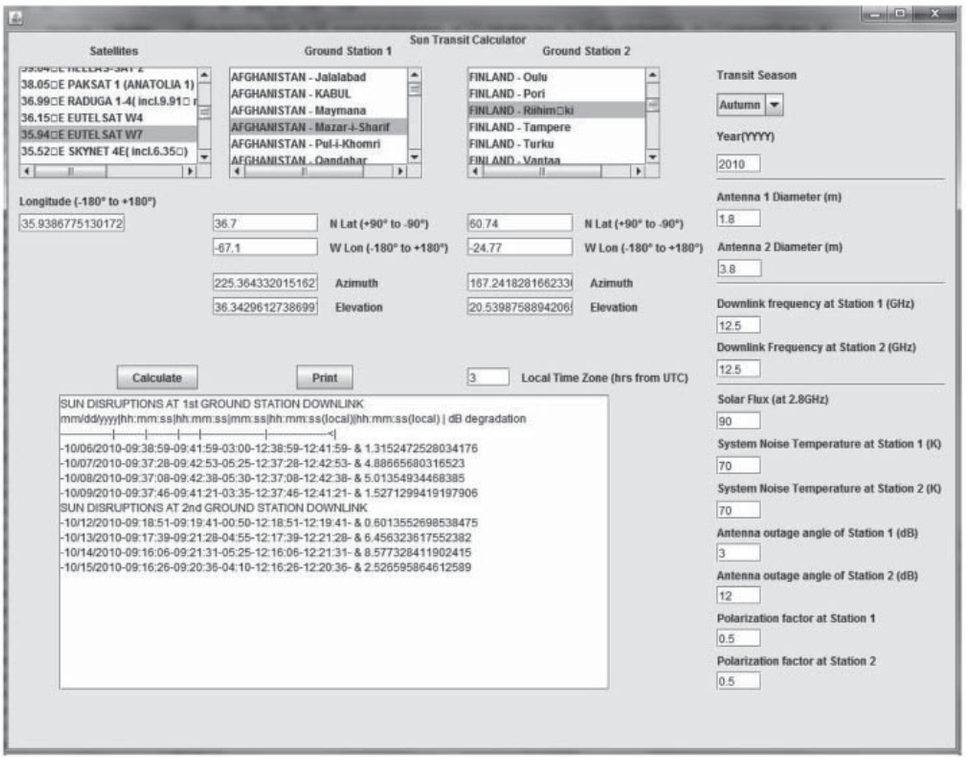

FIGURE 9. The sun outage calculator. After choosing for the particular satellite, receiving ground stations, and feeding the required inputs, the program prints the respective outage times and their associated signal degradation

script, while the actual calculations are performed using JavaScript. The strength of sun outage is calculated from Equation 1-6 (see sun outage strength calculation block in Figure 10). The calculation of the angle between the position of a satellite and the current position of the sun (see Figure 10), and sun outage duration were performed using the Java Astrodynamics Toolkit (JAT) provided by NASA's Goddard Space Flight Center (see sun angular position and outage duration calculation blocks in Figure 10). The JAT library and its necessary functions are invoked from the JavaScript.

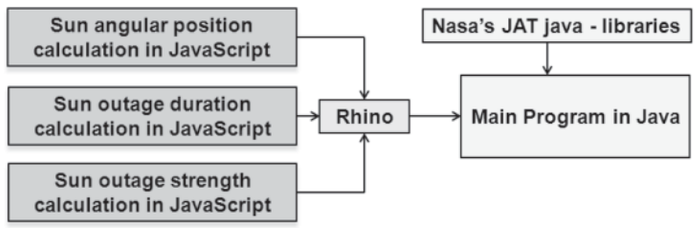

FIGURE 10. A structural representation of the design of the calculator in terms of the various libraries, languages, and interfaces used

MEASUREMENT RESULTS

MEASUREMENT ARRANGEMENTS

The predicted results given by the developed program were compared to measured ones during sun outages at two ground stations (Figure 11): Afghanistan (with an antenna diameter of 1.8 m, Table 2), Finland (with an antenna diameter of 3.8 m, Table 3 and Table 4) and Djibouti (with an antenna diameter of 1.8 m, Table 5).

Table 2 shows the sun outage strength and duration results measured in Afghanistan and those predicted by the program. Table 3, in turn, shows the same two batches of results for Finland (Vankka 2009). Ping tests (sending a package regularly to the target and back) were used to measure the actual duration of the outage. Table 4 and Table 5 show the sun outage strength and duration results measured in Finland and Djibouti for a C-band with an antenna diameter of 3.8 m and 1.8 m, respectively. The measurement arrangements are similar to those in Figure 11, but the satellite was the 4.98°W Atlantic Bird 3.

K_U-BAND RECEIVER

The Afghanistan end had an adequate $\Delta E_b/N_0$ margin (6.7 dB), using more signal coding and a higher satellite direction gain, and so an approximately 5.5 dB sun outage noise hike did not disrupt the ping test (Table 2). The predicted sun outage in Table 2 differs somewhat, mainly due to the fact that the receiver noise temperature T_{sys} is difficult to measure, as it is dependent on not only on the receiver electronics, but also

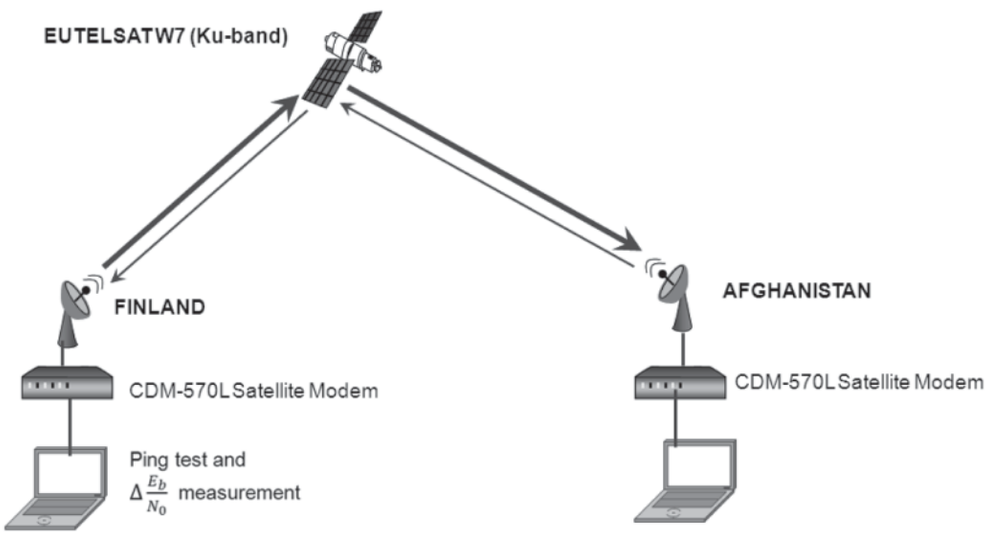

FIGURE 11. Measurement arrangements

TABLE 2. Location of Ground Station: Afghanistan (Satellite: 35.94°E EUTELSAT W7)

Date	Outage start (UTC)	Predicted outage duration (3dB) (min)	Outage duration (min)	Ping test disrupted (min)	$\Delta\left(\frac{E_B}{N_o}\right)$ margin (dB)	Predicted outage $\Delta\left(\frac{E_B}{N_o}\right)$ (dB)	Measured outage $\Delta\left(\frac{E_B}{N_o}\right)$ (dB)
10/7/2010	9:37:38 AM	5.25	05:05	-	6.7	4.88	4.7
10/8/2010	9:37:12 AM	5.30	05:20	-	6.7	5.00	5.1

TABLE 3. Location of Ground Station: Finland (Satellite: 35.94°E EUTELSAT W7)

Date	Outage start (UTC)	Predicted outage duration (3dB) (min)	Predicted outage duration (min)	Ping test disrupted (min)	$\Delta\left(\frac{E_B}{N_o}\right)$ margin (dB)	Predicted outage $\Delta\left(\frac{E_B}{N_o}\right)$ (dB)	Measured outage $\Delta\left(\frac{E_B}{N_o}\right)$ (dB)
10/12/2010	9:18:30 AM	-	01:05	02:48	0.5	0.82	-
10/13/2010	9:17:39 AM	02:55	04:55	05:57	0.5	8.35	-
10/14/2010	9:16:58 AM	03:45	05:30	07:48	0.5	12.00	-

on the temperature seen by the antenna beam. The duration of the sun outage was predicted using a 3-dB outage angle (see Figure 8).

The predicted sun outage at the Finnish ground station (Table 3) is stronger (though shorter in duration) than the one in Afghanistan (Table 2) due to the larger antenna diameter employed at the station. The measured $\Delta E_b/N_0$ dropped to zero (the last column in Table 3), so no results were obtained of the actual strength of the sun outage. The $\Delta E_b/N_0$ margins shown in Table 3 were not adequate to keep the connection going with the powerful outage that hit the beam of the antenna. The duration of the sun outage was predicted using two different outage angles (see Figure 8), 3 dB and 12.3 dB. The predicted outage durations in Table 3 were shorter than those measured using ping tests, which can be explained by the time taken for the modem to recover and the connection to be re-established. The outage angle (12.3 dB) (Table 3, column 4) is calculated from the maximum predicted $\Delta E_b/N_0$ minus the $\Delta E_b/N_0$ margin (Table 3, column 6); this process has better predictive value for sun outage duration than does the outage angle (3 dB). In addition, the outage occurring at 10/12/2010 couldn't be predicted with a 3-dB outage angle (see Table 3), as the $\Delta E_b/N_0$ margin was relatively low and even a disruption source that was far away from the center point of the antenna's beam was able to break the connection.

C-BAND RECEIVER

The C-band receiver (Table 4) will have longer sun outage durations than the K_u-band receiver (Table 3), which can be explained by the narrower beam width of the Ku-band antenna (the antenna diameter of 3.8 meters, Table 3 and Table 4). The $\Delta E_b/N_0$ measured dropped to zero (the last column in Table 4), so no results were obtained for the actual strength of the sun outage. The outage angle (2.9 dB) (Table 4, column 3) is calculated from maximum predicted $\Delta E_b/N_0$ minus $\Delta E_b/N_0$ margin (Table 4, column 6), which more accurately predicts sun outage durations (ping tests) than does the outage angle (12 dB). Inaccuracies in antenna pointing and errors in the knowledge of the exact solar flux value could explain that the outage occurring on 2/27/2011 had a shorter measured outage period than that occurring on 3/1/2011, even though it had a more powerful predicted outage strength.

TABLE 4. Location of Ground Station: Finland (Satellite: 4.98°W ATLANTIC BIRD 3)

Date	Outage start (UTC)	Predicted outage duration (2.9dB) (min)	Predicted Outage duration (12dB) (min)	Ping test disrupted (min)	$\Delta\left(\frac{E_B}{N_o}\right)$ margin (dB)	Predicted outage $\Delta\left(\frac{E_B}{N_o}\right)$ (dB)	Measured outage $\Delta\left(\frac{E_B}{N_o}\right)$ (dB)
2/26/2011	00:40:14 PM	04:40	06:55	04:04	8.9	9.11	-
2/27/2011	00:39:02 PM	06 :50	08:35	06:26	8.9	10.68	-
2/28/2011	00:38:25 PM	07:20	09:00	07:23	8.9	11.40	-
3/1/2011	00:38:06 PM	06:35	08:20	07:20	8.9	10.54	-

The sun outage at the Finnish ground station (Table 4) is stronger (though shorter in duration) than the one at the Djibouti station (Table 5) due to the larger antenna diameter employed in Finland. The outage angle (4.5 dB) is calculated from the maximum predicted $\Delta E_b/N_0$ minus $\Delta E_b/N_0$ margin (Table 5, column 6), which in turn more accurately predicts sun outage durations than does the outage angle (12 dB).

TABLE 5. Location of Ground Station: Djibouti (Satellite: 4.98°W ATLANTIC BIRD 3)

Date	Outage start (UTC)	Predicted outage duration (4.5dB) (min)	Predicted Outage duration (12dB) (min)	Ping test disrupted (min)	$\Delta\left(\frac{E_B}{N_o}\right)$ margin (dB)	Predicted outage $\Delta\left(\frac{E_B}{N_o}\right)$ (dB)	Measured outage $\Delta\left(\frac{E_B}{N_o}\right)$ (dB)
3/15/2011	00:50:37 PM	15:55	24:55	16:23	1.8	6.20	-
3/16/2011	00:48:54 PM	16:00	25:00	17:53	1.8	6.23	-

CONCLUSION

The effect of the downlink frequency (C-band and K_u-band), receiver antenna aperture diameter, and antenna pointing offsets on the duration and strength of disruptions of satellite communications due to sun outages were investigated by simulations and measurements. The sun outage is stronger (though shorter in duration) as the antenna aperture diameter and downlink frequency increase (increasing antenna gain).

Several calculation tools exist in the public domain that can be used to predict the strength and time parameters of a solar outage between geostationary satellites and ground station locations. These tools make various assumptions that adversely affect the quality of the sun outage prediction. An example of such an assumption is their use of a fixed 3 dB outage angle, giving predictions with incorrect duration times or missing outages completely (see Table 3). The sun outage calculator presented in this paper has several key inputs available, such as the solar flux and the outage angle, which enables more efficient calculation of sun outage strength and duration times.

REFERENCES

Bruevich, E. A., Bruevich, V. V. & Yakunina, G. V. 2014. Changed relation between solar 10.7-cm radio flux and some activity indices which describe the radiation at different altitudes of atmosphere during cycles 21-23. *Journal of Astrophysics and Astronomy* 35(1): 1-15.

Cakaj, S., Keim, W. & Malaric, K. 2005. Sun noise measurement at low Earth orbiting satellite ground station. *Proceedings of 47th International Symposium ELMAR*: 345-348.

Garcia, H. A. 1984. Geometric aspects of solar disruptions in satellite communication. *IEEE Transactions on Broadcasting* 30(2): 44-49.

Guo, Y., Li, M., He, S., Xin, P. & Tao, L. 2012. Analysis of the Sun Transit Outage Impact on the Inter-satellite Link of the Navigation Satellite. *Proceedings of China Satellite Navigation Conference (CSNC) 2012*: 133-143.

Ho, C., Slobin, S., Kantak, A. & Asmar, S. 2008. Solar brightness temperature and corresponding antenna noise temperature at microwave frequencies. *IPN Progress Report 42-175*: 1-11. http://ipnpr.jpl.nasa.gov/progress_report/42-175/175E.pdf.

Johannsen, K. G. 1988. Combating sun outage in satellite television distribution systems. *IEEE Transactions on Broadcasting* 34(1): 18-23.

Kivaria, S., Tarimo, C., Hamad, O. F. & Marwala, T. 2011. Computerized fault monitoring and management subsystem with critical solutions archival capabilities in a satellite earth station. *Proceedings of the 10th WSEAS international conference on communications, electrical & computer engineering, and 9th WSEAS international conference on Applied electromagnetics, wireless and optical communications*: 210-220.

Lyon, D. & Mohammed, F. 1998. Effects of solar transit in K_u-band VSAT systems. *IEEE Transactions on Communications* 36(7): 892-894.

Mcgrath, K. M. 2002. Calibration of the Doppler on wheels system gain using solar flux. http://weather.ou.edu/~kmcgrath/ITSkills/Latex/radar.pdf.

NGDC. 2013. Solar Data Services, Penticton/Ottawa 2800 MHz Solar Flux (National Geophysical Data Center). http://www.NGDC.noaa.gov/stp/space-weather/solar-data/solar-features/solar-radio/noontime-flux.

Siocos, C. A. 1973. Broadcasting-satellite coverage-geometrical considerations. *IEEE Transactions on Broadcasting* 19(4): 84-87.

Song, Y., Kim, K-S., Jin, H. & Lee, B-S. 2010. Prediction of communication outage period between satellite and Earth station due to Sun Interference. *Journal of Astronomy and Space Sciences* 27(1): 31-42.

Sun Outage Calculator. 2013. [Online]. http://www.satellite-calculations.com/SUNcalc/SUNcalc.htm [23 Nov 2013].

Telesat Sun Outage Calculator. 2013. [Online]. Available: https://support.telesat.ca/SunTransit/ [23 Nov 2013].

Vankka, J. 2009. Concept of Finnish Defence Forces SatCom CRO (Crisis Management Operations). *Proceedings of Global MilSatCom 2009 Conference*.

Vankka, J. & Kestila, A. 2013. Sun outage calculator for satellite communications. *Proceedings of IEEE International Conference on Space Science and Communication (IconSpace)*: 51-55.

Vuong, X. T. & Forsey, J. 1983. Prediction of sun transit outages in an operational communication satellite system. *IEEE Transactions on Broadcasting* 29(4): 121-126.

Wenjuan, J. & Peng, Z. 2010. Prediction and compensation of sun transit in LEO satellite systems. *Proceedings of 2010 International Conference on Communications and Mobile Computing (CMC):* 495-499.

*Jouko Vankka
Department of Military Technology
National Defence University
P.O. Box 7
Helsinki, Finland

Antti Kestilä
Faculty of Radio Science and Engineering
Aalto University School of Science and Technology
Helsinki
P.O. Box 11000, FI-00076
Aalto, Finland

*Corresponding author; email: jouko.vankka@mil.fi

Received date: 7th July 2014
Accepted date: 4th October 2014